MICROMECHANICAL MODELS FOR PULTRUDED COMPOSITE BEAMS

E. J. Barbero[1] and S. S. Sonti[2]
Constructed Facilities Center
Department of Mechanical and Aerospace Engineering
West Virginia University
Morgantown, WV 26506-6101

Abstract

Pultrusion is a low cost, mass production processing technique of fiber reinforced composite materials. Pultrusion produces standard structural sections (I-beams, box-beams, cellular sections, etc.). Variability and defects of pultruded materials need to be considered in the experimental methods used to validate micromechanical models and to obtain material property data. In this paper we investigate existing micromechanical models and their applicability to pultruded materials. We develop experimental data on tension and shear to correlate with micromechanical predictions. We select and adapt experimental procedures useful for this particular class of materials. We present correlations between the micromechanical analysis and experimental data for pultruded structural shapes.

1. Introduction

Composite materials have many advantages over conventional materials. Light weight, corrosion resistance, reduced part count, are only a few examples. Most prominent is the chance of creating the best material for each particular application. However, use of composites in structural applications is limited by the high cost of the material and processing of non standardized parts. In this paper we look at pultrusion, which is a low cost, mass production processing technique of standard structural sections. Recent advances in pultrusion technology make possible cost-competitive production of new materials using Epoxies, Graphite, Kevlar, and S-Glass fibers. Current standard structural shapes use less expensive E-Glass and Polyester or Vinylester resins. They are marketed for infrastructural applications that require corrosion resistance and/or to avoid electromagnetic interference. Unlike composites produced with highly controlled processing techniques, pultruded materials have defects proper of a mass production operation. Therefore, we need to address the variability of the material both in the formulation of micromechanical models and in the experimental methods used to validate those models and to obtain material property data.

In order to realize the full potential of composites we need to design the material concurrently with the structure. It is thus necessary to count with analytical models to explore a broad spectrum of resins, fiber systems and fiber orientations. The structural characteristics of interest are stiffness[1], strength[2] , buckling resistance[3] , etc. These structural properties depend on the material system (composite) and the shape of the cross-section of the members. Predicted properties allow us to address the optimization of the material to improve the buckling, crippling, and post-buckling behavior which ultimately control the ultimate bending strength.

The strength-to-stiffness ratio of composites is much larger than for aluminum or steel. Therefore, deflections are of major concern to the structural designer, including axial stiffness, bending stiffness and shear stiffness (shear deformation plays a significant role in the transverse deflections of composite beams). Although we can measure stiffness for existing pultruded members, prediction of properties allows us to optimize the material to make it competitive with conventional materials. Using lamination theory we can predict stiffness properties from the product description used for manufacturing. This includes the material properties of the constituents (fiber and matrix), the orientation and volume fraction of the fibers at different locations on the section (web or flanges), and the shape of the cross-section. Analytical models for stiffness, buckling, and strength depend on accurate micromechanical predictions of the material properties.

Micro-mechanics allows us to relate changes in the material systems to changes in the material properties. In this paper we investigate existing micromechanical models and their applicability to pultruded materials. We develop experimental data on tension and shear to correlate with micromechanical predictions. We select and adapt experimental procedures useful for this particular class of materials. We present correlations between the micromechanical analysis and experimental data for pultruded structural shapes.

Other studies[4] presented experimental data obtained directly from full-size tests of currently produced structural shapes. They addressed the determination of beam bending stiffness including the contribution of shear deformations. These can be input into Timoshenko beam theory for computation of deflections. In this work we look at the validation of micromechanical models that allow to predict those properties among other material properties needed from the description used in manufacturing, thus allowing us to optimize the material for specific applications. The manufacturer's description include a detailed profile of the properties through the

[1] Assistant professor, member ASME

[2] Graduate research assistant

cross section, which is also useful for stress computations. Also, based on micro-mechanics, we predict plate stiffness of the webs and flanges, necessary for crippling analysis. Micro-mechanics allow us to avoid costly experimentation to characterize a continuously growing list of standard shapes (more than 300 different sections from one manufacturer alone). Finally, micro-mechanical models allow us to predict the behavior of future material combinations and thus to optimize their performance by proper design.

2. Modelling of Pultruded Structural Shapes

Fiber reinforced composite beams and columns are inhomogeneous for two reasons. First, the fiber reinforced composite material is inhomogeneous and anisotropic due to the presence of the fibers (glass, kevlar, graphite). Next, different portions of the cross-section are built with different orientation of the fibers, different fiber volume fractions, different fiber systems, etc. This is true not only from a point to point basis (e.g. roving, nexus, continuous strand layers) but also at a larger scale the flanges and webs are usually built with different fiber combinations.

Although pultruded beams are not manufactured by lamination, they do contain different material combinations through the thickness, thus justifying the use of lamination theory. Using micro-mechanics, each layer is modelled as an homogeneous equivalent material that macroscopically behaves similarly to the fibrous composite. With the results from micro-mechanics, lamination theory is used to model an entire flange or web as a yet equivalent homogeneous material. Finally, flanges and webs are assembled into a structural shape obtaining properties useful for structural design[5,6].

3. Micromechanical Models For Pultruded Composite Beams

Considering transverse isotropy on each layer[7] we need four material properties per layer. Using micro-mechanics we determine the material properties for each lamina (E_1, E_2, ν_{12}, G_{12}) from the material properties of fiber (E_f, ν_f) and matrix (E_m, ν_m).

3.1. Determination of Fiber Volume Fraction

The fiber volume fraction V_f is the ratio of the volume of fiber to the total volume of the final product. We compute V_f as the quotient of the area of fibers in the cross-section to the total area of the cross-section. The area A of fibers in the cross section depends of the number of roving n and their yield y [number of yards (0.9144 m) of roving weighing one pound (0.454 Kg)] as

$$A = n / (2.016 . y . \rho) \qquad (1)$$

with A in m^2, ρ in Kg/m^3, and y in yards/lb. For the continuous strand mat (OC), the fiber volume fraction can be computed as

$$V_f^{oc} = \frac{W}{\rho t_c} \qquad (2)$$

where t_c is the thickness of the layer, ρ is the density of the fibers and W is the weight per unit area of the OC mat.

3.2 Tensile Modulus.

In the elasticity solutions with contiguity[7], we assume that either a) fibers are contiguous (i.e., fibers touch each other) or b) fibers are isolated (i.e., fibers are completely separated by resin). If C denotes the degree of contiguity, then C=0 corresponds to isolated fibers and C=1 corresponds to perfect contiguity. For low fiber volume fraction pultruded composites we use C=0. For the material under study we use: E_f = 72.393 GPa, E_m = 3.445 GPa[8] and[7] ν_f = 0.22, ν_m = 0.35. Due to the high tension that pultrusion exerts on the fibers we adopt a fiber misalignment factor K=1. Using Eq. 3.69, 3.66, and 3.67 from[7] we obtain the material properties of each lamina (E_1, E_2, and ν_{12}).

As an example consider a E-Glass-Vinylester pultruded material with V_f=0.25. Using the elasticity approach we obtain: E_1 = 20.632 GPa, E_2 = 4.860 GPa, ν_{12} = 0.313. Using the mechanics of materials approach (Sect. 3.2,[7]) we obtain: E_1 = 20.632 GPa, E_2 = 4.433 GPa, and ν_{12} = 0.318. The prediction of E_1 form both methods coincide because of the value of the fiber misalignment factor. These predictions correlate very well with experimental data.

Pultrusion produces a laminate with all the lamina perfectly bonded together. Therefore, we can only test a laminate. The laminated structure of pultruded materials is an valid idealization as we demonstrate in Sect. 3. In order to compare micromechanical predictions with experimental data we need to determine laminate properties. We accomplish this by using lamination theory. We compute the stiffness matrix for each lamina (Eq. 2.61,[7]) and rotate it to structural axis (Table 3.2,[9]).

Then we compute the extensional stiffness matrix (Eq. 2.41[7]) and invert it to obtain the compliance matrix. Finally we obtain the equivalent material properties for a laminate (Eq. 4.18[9]) that we compare to experimental data in the following section.

3.2.1. Experimental results. We performed tensile tests on coupons cut from 8x8x0.375" (20.32x20.32x0.95 cm) I-beams. We cut various sizes from the webs and flanges of an I-beam (Fig. 1) and we measured longitudinal and transverse strains to compute longitudinal (E_x) and transverse (E_y) tensile moduli.

We performed tensile tests on 45.72x5.08 cm specimen with aluminum tabs on the specimen ends (12.70x5.08 cm) to prevent the grips from damaging the material

during the test. We recorded strains in the longitudinal (fiber) direction, transverse direction and 45°. We tested five specimen, four from the flanges (see Fig. 1) and one from the center of the web. By linear regression on the linear portion of the load-strain curve we obtained the results reported in Table 1.

We performed tensile tests on smaller specimens (20.32x2.54 cm) from the same I-beam on an Instron universal testing machine hooked to a Data Acquisition system. We tested twelve specimen, eight from the flanges and four from the webs . There is noticeable scatter in the values of the elastic moduli. This is due to variability of the material from point to point in the cross-section. Specimen from the intersection of the flanges and the web have lower modulus. This in turn is due to the variability of the fiber volume fraction in that region. Table 2 summarizes the results.

We obtained five transverse specimen (8.89x2.54 cm) from the same beam to determine the transverse tensile modulus,four from the flanges and one from the web. Table 3 summarizes the results.

The elasticity approach to micro-mechanics seems to provide the best predictions for pultruded composite materials.

3.3. Shear Modulus.

We use the elasticity solutions with contiguity for the determination of the shear modulus. Using Eq. 3.68 in Ref. 7 we obtain G_{12} = 1.985 GPa. The predicted value does not correlate well with experimental data. Therefore, we use stress partition parameter[9]. We obtain the stress partition parameter using experimental data for currently produced pultruded material and assume that remains constant while varying the fiber volume and resin properties during material optimization studies.

Iosipescu Shear test. To determine the shear modulus we used the Iosipescu Shear Test Method, originally developed for isotropic materials[10] and used for pultruded composites by Bank[11]. Researchers at Wyoming University redesigned the fixture to be used for composite materials[12,13,14,15]. We built a similar fixture at West Virginia University. We obtained the specimen from the same wide-flange beams used through this study. The specimen is 7.62 cm long and 1.91 cm wide with a 90° notch at the center of the specimen milled with a precision grinding and cutting machine. The notch root radius is 0.13 cm and the notch depth is equal to 20% of the specimen width. We use an Instron universal testing machine in compression mode and record the results using a Data Acquisition system. Fig. 2 represents a typical stress-strain curve where the nonlinearity of the shear modular is apparent. We tested nine specimen, six from the flanges and three from the web. Again, there was noticeable scatter due to the variability of the material. The Iosipescu test gives the shear modulus of a small region of the material. An average of the values obtained at several locations on the cross section of the beam seems to be a good estimate as suggested by the torsion results that we describe next. The values for the shear modulus using this method are higher than the micro-mechanics prediction, which is not accurate in this case. The values of the shear modulus obtained by linear regression on the load-strain curves from a two-element strain gage are given in Table 4.

3.3.2. Torsion test. The Iosipescu test results show a large scatter due to the variability of the pultruded material from point to point in the cross-section of the structural shape. Therefore, we used a torsion test[16,17] that allows us to test larger samples. For this test we assume transverse isotropy of the laminate[18]. The shear modular can be computed from Lekhnitskii torsion solution for orthotropic rectangular bars.

$$K = \frac{T}{\theta} = \frac{G_{12} d t^3}{L} \frac{1}{\beta} \qquad (3)$$

with d t = cross-sectional area, L = gage length ($L < L_o$), T = torque, θ = twist angle (Fig. 3), where

$$\beta = \beta(G_{12}, G_{13}) \qquad (4)$$

and assuming $G_{12} = G_{13}$ or performing tests for two different cross sections. We tested four samples (43.18x2.54 cm) form the four flanges of the same I-beam and one sample from the web (Fig. 1). We computed the moment from the displacement of the reacting arm, displacement that we measured by a LVDT hooked to a data acquisition system. We measured the twisting angle on a gage length of 27.94 cm as the difference between two LVDT hooked to the DAS. The loading rate was less that 3° per minute both in loading and unloading. To asses the effect of possible misalignment we applied both clockwise and counter clockwise twisting. Fig. 4 represents a typical torque us angle of twist curve. The apparent histeretic effect is not due to the material but to the statis friction of the hubs on the torsion machine. The curves are linear due to the low strain level experienced in the material during test. Table 5 summarizes the results.

We conclude that the torsion test results are approximately the average of the Iosipescu results. This fact confirms that the variability of the material is responsible for the scatter in the Iosipescu results. The torsion test averages the values of the shear moduli over a large area (27.94x2.54 cm). Therefore we recommend the use of the torsion test to characterize the structural behavior of the pultruded beams. Furthermore, the Iosipescu method requires the use of costly and cumbersome strain while the torsion method uses simpler LVDT. However, the Iosipescu method provides the shear strength, while the torsion method does not. We are developing a torsion failure criteria that will

allow us to use the torsion method for determination of shear strength.

3.4. Compression properties

Gurdal[19] developed a compression test fixture at Virginia Polytechnic Institute and State University. We built a similar one, adapted for larger samples required for this work. The advantages of this fixture over the existing fixtures are 1) ease of specimen preparation, 2) ease of specimen alignment, 3) longer test section, 4) reduction of stress concentrations, 5) ease of specimen stress analysis, and 6) prevention of buckling of the coupon at higher loads. Results of compression tests will be presented and compared to full size compression tests currently under way.

4. Conclusions

The elasticity approach to micro-mechanics seems to provide the best predictions for pultruded composite materials. Longitudinal and transverse moduli and Poisson ratio predictions correlate very well with experimental data. Shear modulus was under-predicted. The stress partition parameter is needed to obtain reallistic predictions of the shear modulus to be used in material optimization. Due to the variability of the material, large samples give results that are more representative of the structural behavior. This is specially true for shear, where the torsion test gives more consistent results than the Iosipescu test.

5. References

1. Barbero, E.T., *"Pultruded Structural Shapes - From the Constituents to the Structural Behavior,"* SAMPE Journal, Jan. 1991a.

2. Barbero, E. J. and Fu, S. H.,*"Local Buckling as Failure Initiation in Pultruded Composite Beams,"* ASME Winter Annual Meeting, 1990a.

3. Barbero, E. J. and Raftoyiannis, I., *"Laminated Beam Theory for Complex Composite Sections,"* CFC Report, West Virginia University, August 1990c.

4. Bank, L. C., *"Properties of Pultruded Fiber Reinforced Plastic (FRP) Structural Members,"* paper 880501, 68th Annual Meeting, Transportation Research Board, January 22-26, 1989. Washington, DC.

5. Tsai, S. W., Composites Design, 4th Ed., Think Composites, 1989.

6. Barbero, E. J. ,*"Pultruded Structural Shapes: Stress Analysis and Failutre Prediction,"* ASCE Specialty Conference on Advanced Composites in Civil Engineering Structures, Las Vegas, Nevada, Jan. 1991b.

7. Jones, R. M., Mechanics of Composite Materials, Hemisphere Publishing Corporation, 1975.

8. Creative Pultrusions Design Guide, Creative Pultrusions Inc., Pleasantville Industrial Park, Alum Bank, PA 15521.

9. Tsai, S. W. and Hahn, H. T., Introduction to Composite Materials, Technomic Publishing Co., 1980.

10. Iosipescu, N., *"New Accurate procedure for Single Shear Testing of Metals,"* Experimental Mechanics, 2(3), 537-566, 1967.

11. Bank L.C. *"Shear Properties of Pultruded Glass FRP Materials"* ASCE Structures congress'89, May 1-5, 1989, San Francisco, CA.

12. Spigel B.S.,Prabhakaran R.,and Sawyer J.W. *"An investigation of the Iosipescu and Asymmetrical Four-Point Bend Tests,"* Experimental Mechanics 27(1), 57-63, March 1987.

13. Adams, D. F. and Walrath, D. E., *"Verification and Application of the Iosipescu Shear Test Method,"* Rep. No. UWME-DR-401-103-1,Dept. of Mechanical Engineering, Univ. of Wyoming, NASA Grant No. NAG-1-272, June 1984.

14. Adams D.F. and Walrath D.E. *"Further Development of the Iosipescu Shear Test Method,* "Experimental Mechanics 27(2), 113-119, June 1987.

15. Arcan M. *"The Iosipescu Shear Test as Applied to Composite Materials,"* Experimental Mechanics, 24(1), 66-67, March 1984.

16. Cohen, D., *"Effects of Thermal Cycling on Matrix Cracking and Stiffness Changes in Composite Tubes,"* M.S. Thesis, Virginia Polytechnic Institute and State University, 126-129, August 1984.

17. Semenov, P. I., *"Determination of shear moduli of Orthotropic Materials from Torsion Tests,"* Mekhanika Polimerov, 2 (1), 27-33, 1966.

18. Davalos, J. F., Loferski, J. R., Holzer, S. M., and Yadama, V., *"Transverse Isotropy Modelling of 3-D Glulam Timber Beams,"* ASCE Journal of Materials in Civil Engineering, 1990.

19. Gurdal, Z. and Starbuck, J. M., *"Compressive Characterization of Unidirectional Composite Materials,".*

Table 1: Longitudinal tension test results from large samples.

Location	E_x (GPa)	ν_{12}
Flange 1	18.615	0.29
Flange 2	19.994	0.29
Flange 3	22.062	0.35
Flange 4	19.994	0.23
Web 1	15.168	0.19

Table 2: Longitudinal tension test results.

Location	E_x (GPa)	ν_{12}
Flange 5	22.752	0.279
Flange 6	20.408	0.278
Flange 7	18.753	0.300
Flange 8	12.824	0.244
Flange 9	15.512	0.291
Flange 10	27.578	0.230
Flange 11	16.891	0.288
Flange 12	18.201	0.299
Web 2	15.650	0.280
Web 3	15.444	0.277
Web 4	16.340	*[3]
Web 5	16.478	0.280

Table 3: Transverse tension test results.

Location	E_y (GPa)	ν_{21}
Flange 13	5.791	0.26
Flange 14	6.067	0.13
Flange 15	4.412	0.14
Flange 16	5.929	0.23
Web 6	4.136	0.14

Table 4: Iosipescu test results.

Location	G_{xy} (GPa)
Flange 17	4.964
Flange 18	4.329
Flange 19	2.861
Flange 20	2.502
Flange 21	2.357
Flange 22	3.923
Web 7	4.626
Web 8	4.412
Web 9	3.481

Table 5 : Torsion test results

Location	Twisting	Loading G (GPa)	Unloading (GPa)
Flange 1	Clockwise	3.658	3.618
Flange 1	Counterclockwise	3.809	3.831
Flange 2	Clockwise	3.749	3.890
Flange 2	Counterclockwise	3.963	4.059
Flange 3	Clockwise	3.854	3.855
Flange 3	Counterclockwise	3.959	4.095
Flange 4	Clockwise	3.518	3.517
Flange 4	Counterclockwise	3.712	3.736
Web 1	Clockwise	3.810	3.826
Web 1	Counterclockwise	3.945	4.018

[3] not recorded

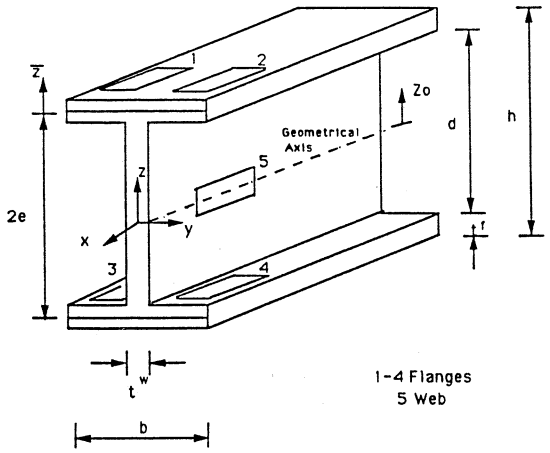

Figure 1

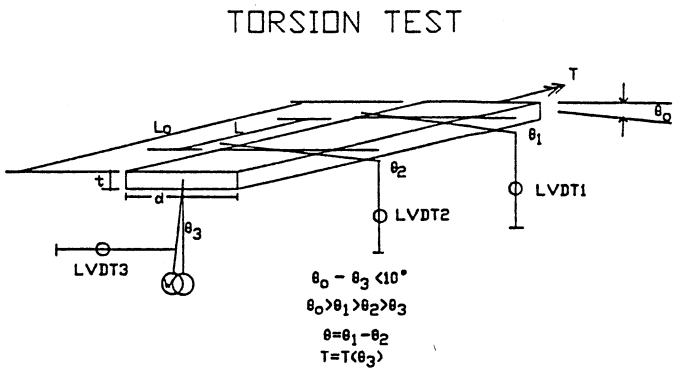

Figure 3

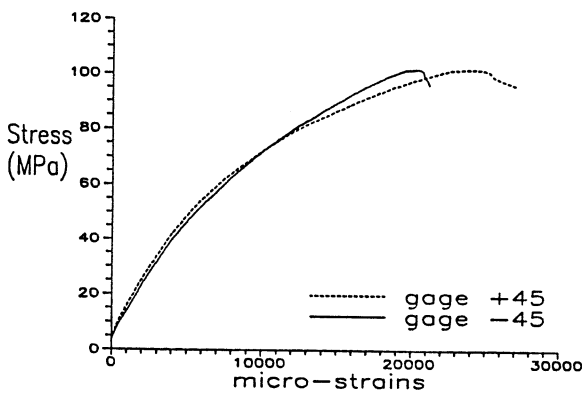

Figure 2

Figure 4